RAPID COMMUNICATIONS

PHYSICAL REVIEW B VOLUME 48, NUMBER 8 15 AUGUST 1993-I

Energy-band renormalization and energy-relaxation dynamics of the X_6 and X_7 satellite valleys in GaAs

M. A. Cavicchia and R. R. Alfano

Institute for Ultrafast Spectroscopy and Lasers, Physics Department, The City College and The Graduate School of the City University of New York, New York, New York 10031

(Received 30 April 1993)

Using femtosecond UV-pump–IR-probe absorption spectroscopy, energy-band renormalization of the X_6 and X_7 satellite conduction-band valleys and energy relaxation of electrons in the X_6 and X_7 valleys by intervalley scattering, $X_6 \leftrightarrow \Gamma$ and $X_7 \leftrightarrow \Gamma$, as a function of photoexcited electron density, were observed in GaAs. The measured energy renormalization and its density dependence are compared with theory. It is determined that $X_7 \rightarrow \Gamma$ intervalley scattering is faster than $X_6 \rightarrow \Gamma$ intervalley scattering.

Knowledge of the electron dynamics and band-structure properties of the satellite X valleys is important in determining the high-field transport properties of GaAs. $\Gamma \rightarrow X$ intervalley transfer has been shown to be the dominant energy-relaxation mechanism for high-energy, photoexcited electrons.[1] A Monte Carlo calculation by Sánchez *et al.*,[2] which employs a five-valley conduction-band model, reveals the strong influence of the X_7 valley regarding transport phenomena in the high-field range. Band-gap renormalization (BGR) is a well-known phenomenon that occurs in semiconductors with high densities of photogenerated carriers.[3] A reduction of the fundamental, direct or indirect, band gap, due to exchange and correlation forces between the carriers,[4] has previously been observed in GaAs (Ref. 5) and $Al_xGa_{1-x}As$,[6] but there have been no measurements of BGR of the upper satellite conduction bands. Kalt and Rinker[7] (KR) have analyzed BGR in semiconductors with multiple inequivalent valleys and have shown that it has a significant effect on the nature of the band structure in semiconductors.

In this paper we report on the measurement of an upper satellite conduction-band-involved intervalley scattering process, $X_7 \leftrightarrow \Gamma$, the observation of energy-band renormalization of the X_6 and X_7 satellite conduction-band valleys, and the observation of the Burstein-Moss shift[8] of the $X_6 \rightarrow X_7$ interband absorption, in highly photoexcited GaAs. These new, general interest observations of the energy relaxation dynamics of high-energy, high-density electrons in the X_6 and X_7 valleys and the effect of the high-density electron-hole (e-h) plasma on the energy-band structure were studied using femtosecond UV-pump–IR-probe absorption spectroscopy.

The setup used to perform these measurements is a modification of a visible-pump–IR-probe setup which has been described previously.[9] A 500-fs UV pump pulse (293 nm) was obtained from the second harmonic of the fundamental laser wavelength (585 nm). A 500-fs tunable IR probe pulse (2.5–5.5 μm) was used to monitor the induced IR absorption. The UV pump and the IR probe pulses were loosely focused onto a 350-μm aperture to obtain fairly uniform intensities across the sample. The sample used was a 4-mm, Czochralski-grown, undoped GaAs crystal at room temperature. Using the intense 293-nm pump pulse, electrons are photoexcited to the upper part of the Γ band. The relaxation dynamics proceed as depicted in the inset of Fig. 1(b). The dominant relaxation mechanism for this case is intervalley scattering to the X_6 and X_7 valleys. Once electrons scatter to the X valleys they then relax by emitting LO phonons which is a more effective relaxation process for valleys with large effective masses.[10] These relaxation processes and electron thermalization in the X valleys take place within the risetime of the induced IR absorption ($\lesssim$ 2 ps). Their effect is to put a large quasithermal population of electrons in the X valleys which will subsequently undergo intervalley scattering back to the lower-energy Γ valley states. This backscattering takes place on a time scale of tens of picoseconds.

The induced IR absorption spectrum was measured as a function of pump fluence at a delay time τ of 2 ps between the pump and probe pulses. At this delay time the density of electrons in the X valleys has reached a maximum and the absorption of the IR probe is at its peak. For the highest pump fluence, we have measured the spectrum as a function of delay time between the pump and probe pulses. The results are shown in Figs. 1(a) and 1(b). The salient feature of the curves in Fig. 1(a) is that as the pump fluence increases not only does the strength of the ir absorption increase, but the onset energy of the $X_6 \rightarrow X_7$ absorption band, indicated in the figure by arrows, decreases. Additionally, notice that there is a shift between the onset of the absorption band and the peak of the absorption band which increases as the pump fluence increases. This is a Burstein-Moss shift which increases with the increasing degeneracy of electrons in the X_7 valley (i.e., band filling). These features will be discussed in detail below.

The solid lines in Figs. 1(a) and 1(b) are a least-squares fit of the spectra using a model that includes contributions to the induced IR absorption from (1) free carrier absorption (FCA) by the photoexcited electrons and holes,[11] (2) direct interconduction band absorption (DIBA) by electrons in the X_6 valley to the X_7 valley,[12] and (3) indirect interconduction band absorption (IIBA)

by electrons in the Γ valley to higher-energy valleys (X_6 or L_6).[11] Intervalence band absorption has been shown to be negligible in comparison to these processes[12] and is excluded from this analysis.

The theoretical fits are obtained by summing the separate contributions to the total induced absorption. In terms of the measured change in optical density,

$$\Delta\mathrm{OD}(\lambda)=\Delta\mathrm{OD}_{\mathrm{FCA}}(\lambda)+\Delta\mathrm{OD}_{\mathrm{DIBA}}(\lambda)+\Delta\mathrm{OD}_{\mathrm{IIBA}}(\lambda)\ . \tag{1}$$

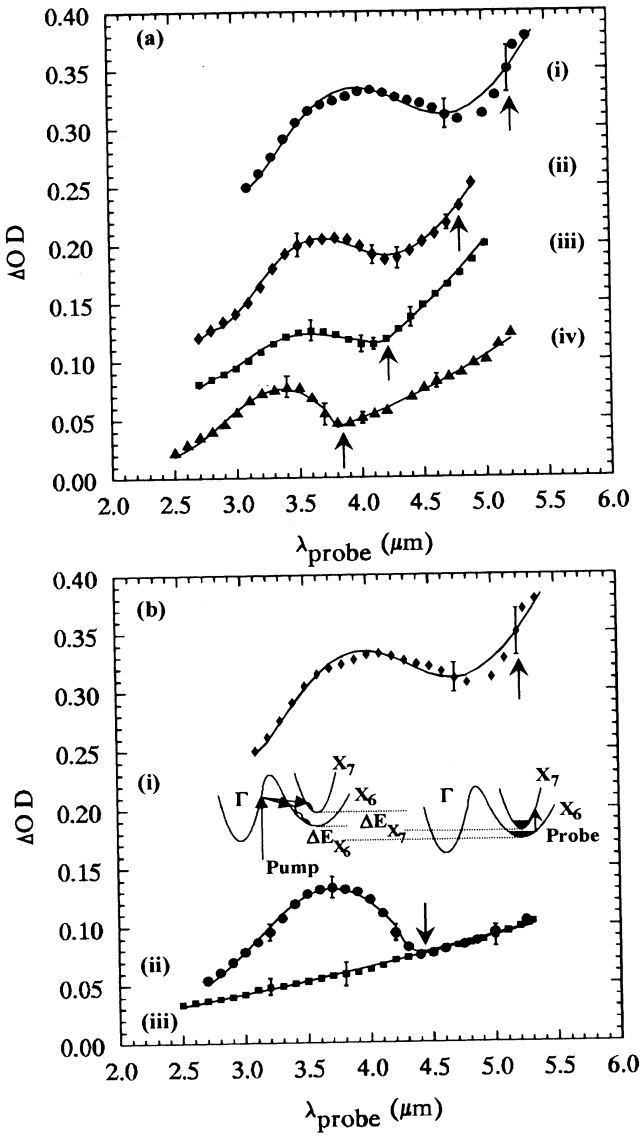

FIG. 1. Induced IR absorption spectra, $\lambda_{\mathrm{pump}}=293$ nm, (a) $\tau=2$ps, as a function of pump pulse fluence: (i) 0.860 mJ/cm^2, (ii) 0.550 mJ/cm^2, (iii) 0.400 mJ/cm^2, (iv) 0.200 mJ/cm^2; (b) pump pulse fluence =0.860 mJ/cm^2: (i) $\tau=2$ ps, (ii) $\tau=20$ ps, (iii) $\tau=60$ ps. Typical error bars are shown. Solid lines are theoretical fits. Arrows indicate onset energy of $X_6\rightarrow X_7$ absorption band obtained from the fit, as explained in the text. Inset is a diagram of the electron energy-relaxation processes and renormalization in the X_6 and X_7 valleys.

The free carrier contribution, which dominates at longer wavelengths, increases linearly with pump intensity and rises as[8] $\Delta\mathrm{OD}_{\mathrm{FCA}}(\lambda)\propto\lambda^p$. The best fit for the spectra at $\tau=2$ ps is given by $p=3.2$ which may indicate strong impurity and optical-phonon scattering, but for later times, at $\tau=20$ and 60 ps the best fit is given by $p=1.5$ which may indicate strong acoustic-phonon scattering.

The direct $X_6\rightarrow X_7$ absorption spectrum of this allowed, momentum-conserving transition is calculated using second-order perturbation theory. The absorption change can be written after integration over k as[12]

$$\Delta\mathrm{OD}_{\mathrm{DIBA}}(\lambda)\propto(hc/\lambda-\Delta E'_{X_6,X_7})^{1/2}m_r^{2/3}\times[f_6(E_6,E_{f6},T_e)-f_7(E_7,E_{f7},T_e)]\ , \tag{2}$$

where f_6 and f_7 are the Fermi-Dirac distributions for electrons in the X_6 and X_7 valleys, respectively, E_{f6} and E_{f7} are the quasi-Fermi energies for the populations in the X_6 and X_7 valleys, respectively, $\Delta E'_{X_6,X_7}$ is the renormalized energy gap between the X_6 and X_7 valley minima, T_e is the electron temperature, and m_r is the reduced effective mass, $m_r=m_6m_7/(m_6-m_7)$, where m_6 and m_7 are the density-of-states effective masses of the X_6 and X_7 valleys, respectively. For GaAs, $m_6=0.85m_e$ and $m_7=0.48m_e$,[12] where m_e is the free-electron mass. The energies of the optically coupled states E_6 and E_7 at the probe wavelength λ can be expressed in terms of the effective masses and $\Delta E'_{X_6,X_7}$ as

$$E_{6,7}(\lambda)=(m_r/m_{6,7})(hc/\lambda-\Delta E'_{X_6,X_7})\ . \tag{3}$$

The second-order process of indirect interconduction band absorption has been successfully used by Jordan[11] to fit the IR absorption data in n-type GaAs of several experimental groups. This indirect absorption dominates the spectrum for λ less than 3.0 μm. It is only necessary to include this process in our model to give a satisfactory fit to our spectra in the high-energy tail of the $X_6\rightarrow X_7$ absorption band. It has no effect on the fit to the main part of the band at wavelengths longer than 3.0 μm. For wavelengths between 3.0 and 2.5 μm this absorption has been shown to rise slowly and has no drop-off at shorter wavelengths. In our analysis, it is not necessary to include this process to fit the case of the lowest pump fluence or for the case of the highest pump fluence at a delay time of 20 ps. For low pump fluence, the contribution is weak because of a low density of electrons in the Γ valley. At high pump fluence, but long delay times, many of the X_6 and L_6 states have been filled by electrons which have relaxed to the bottom of these bands, so the contribution is again reduced.

From our fit to the $X_6\rightarrow X_7$ spectrum we can extract E_{f6} and E_{f7}, T_e, and $\Delta E'_{X_6X_7}$. From E_{f6}, E_{f7}, and T_e, we calculate the electron densities of the X_6 and X_7 valleys, n_6 and n_7, respectively, using the approximation of Aguilera-Navarro, Estévez, and Kostecki.[13] We estimate the total density of carriers n from the pump fluence and from the magnitude of the free carrier absorption. These results are displayed in Table I.

TABLE I. Results of fitting $X_6 \rightarrow X_7$ absorption band for various experimental conditions. $\Delta E'_{X_6,X_7}$(expt) is the renormalized energy gap determined from fitting the spectra and $\Delta E'_{X_6,X_7}$(theory) is calculated using the KR model.

Pump fluence (mJ/cm^2)	Delay (ps)	n (10^{20} cm^{-3})	n_6 (10^{20} cm^{-3})	n_7 (10^{20} cm^{-3})	$\Delta E'_{X_6,X_7}$(expt) (eV)	$\Delta E'_{X_6,X_7}$(theory) (eV)
0.20	2	2.4	1.09	0.096	0.322±0.007	0.309
0.40	2	4.8	1.75	0.233	0.295±0.006	0.300
0.55	2	6.4	4.09	1.270	0.258±0.009	0.262
0.86	2	10.0	7.22	2.730	0.238±0.006	0.233
0.86	20	3.3	1.31	0.090	0.288±0.006	0.301

The arrows in Fig. 1 are placed at the energies $\Delta E'_{X_6,X_7}$, obtained from the fit, which correspond to the onset of the $X_6 \rightarrow X_7$ absorption. At this energy the IR absorption deviates from the power law describing FCA. Even though we have assumed k conservation, there is not a sharp onset of the $X_6 \rightarrow X_7$ absorption due to band filling of the X_7 valley.[5] Carriers at the bottom of the X_7 valley limit the number of final states available for the absorption and shifts the peak of the absorption to higher energy. Lifetime and collision broadening[14] of the $X_6 \rightarrow X_7$ absorption spectra are not needed to obtain a good fit to the data. If included, they may change the values of T_e, n_6, n_7, and $\Delta E'_{X_6,X_7}$ obtained from our fit to the data. In particular, $\Delta E'_{X_6,X_7}$ may be changed by as much as 6 meV, but this is on the order of the uncertainty in our determination of this value. Therefore, we choose to neglect these effects. As will be seen, we still obtain a good agreement with theory.

To explain the observed shift of the onset energy of the $X_6 \rightarrow X_7$ absorption band we follow the procedure of KR (Ref. 7) to calculate the separate renormalizations of the X_6 and X_7 valleys. This procedure accounts for the fact that the electrons experience a Coulomb interaction with all the other electrons and holes regardless of which valley they are in, but they experience an exchange interaction only with other electrons residing in the same valley. The exchange-correlation energy is calculated, first assuming that all the electrons are in a single valley. This is accomplished by using the universal formula derived by Vashishta and Kalia for the exchange-correlation energy of an e-h plasma,[15] $\varepsilon_{xc}(r_s)=[(a+br_s)/(c+dr_s+er_s^2)]\mathrm{Ry}^*$, where Ry* is the excitonic Rydberg, $r_s=(3/4\pi n a_{ex})^{1/3}$ is the dimensionless mean interparticle separation, n is the carrier density, $a_{ex}=(\varepsilon_s\hbar^2/m_{ex}e^2)$ is the excitonic Bohr radius, m_{ex} is the reduced excitonic mass, and ε_s is the static dielectric constant. The coefficients a,b,c,d,e are given in Ref. 15. Then, subtract from ε_{xc} the full electron exchange energy,[4] $E_x^e=-[0.916\phi(\rho_e)/r_s\nu_e^{1/3}]\mathrm{Ry}^*$, where ν_e is the degeneracy of the valley, $\phi(\rho_e)$ is an anisotropy factor, $\phi(\rho_e)=\{\rho_e^{1/6}\sin^{-1}[(1-\rho_e)^{1/2}]/(1-\rho_e)^{1/2}\}\mathrm{Ry}^*$, and ρ_e is the ratio of the transverse to the longitudinal effective mass for the valley. The ratio ρ_e for the X_7 valley is assumed to be the same as that for the X_6 valley. Finally, the electron exchange energy is calculated for each valley individually considering only the population density within that valley, and that is added back to the previous result to obtain ε_{xc} for each valley.

The energy renormalization of each band can be obtained from[3] $E-E'=\varepsilon_{xc}+n\partial\varepsilon_{xc}/\partial n$ where E (E') is the unrenormalized (renormalized) energy minimum of the valley and ε_{xc} is the exchange-correlation energy for the valley. The renormalization of the $X_6 \rightarrow X_7$ energy gap is found from the difference of the renormalizations of the energies of the X_6 and X_7 valleys, $\Delta E'_{X_6,X_7}=\Delta E_{X_6,X_7}-\Delta E_{X_7}+\Delta E_{X_6}$, as shown in the inset of Fig. 1(b). The results of these calculations are shown in Table I. Since the effective mass, and hence the density of states, of the X_7 band is less than that of the X_6 band, its energy is reduced by a larger amount for the densities obtained in this experiment. This causes a reduction of the $X_6 \rightarrow X_7$ energy gap. The calculations are in excellent agreement with the measured gaps for the three highest densities and somewhat in agreement for the lower densities. The unrenormalized gap of 0.345 eV was taken from measurements by Wang *et al.*[12]

Consider the ratio of the calculated densities of the X valley populations, n_7/n_6, and the ratio of the density of electrons in the X valley to the total density of electrons, $(n_6+n_7)/n$, as a function of pump fluence. The ratio $(n_6+n_7)/n$ increases dramatically as the density increases, going from less than 50% for the lower densities to 99% for the highest density. In addition, as the total density increases, the ratio n_7/n_6 increases. These effects can be understood in terms of screening by the high-density electron-hole plasma. As the density of carriers increases ($>10^{18}$ cm^{-3}), the relaxation of energy by the emission of polar-optical phonons is reduced by the screening of the Fröhlich interaction. Intervalley scattering, by emission or absorption of nonpolar-optical phonons via a deformation potential interaction, then becomes the dominant energy-relaxation mechanism. Intervalley transfer to the X valleys will thus increase as the emission of polar-optical phonons is reduced. For higher pump fluences, higher electron temperatures are achieved and the populations of the X valleys become degenerate. This give rise to a higher probability of electrons scattering to the X_7 valley as the pump fluence is increased.

As time proceeds, the population of electrons in the X valleys is depleted by intervalley scattering back to the Γ valley. For the case of pump fluence $=0.86$ mJ/cm^2, shown in Fig. 1(b), after 20 ps the ratio of electron densi-

ty in the X valleys to total electron density has decreased from 0.99 to 0.42. Since the ratio of n_7/n_6 has also decreased from 0.38 to 0.07 it can be inferred from the data that the intervalley scattering rate for $X_7 \rightarrow \Gamma$ is faster than that for $X_6 \rightarrow \Gamma$. This observation is supported by (1) the calculated deformation potential constant for scattering between the X_7 and Γ valleys is higher than for scattering between the X_6 and Γ valleys,[16] and (2) the density of states at the point in the Γ valley which the electrons scatter to from the X_7 valley is higher than that at the point which the electrons scatter to from the X_6 valley. The intervalley scattering time for $X_6 \rightarrow \Gamma$ has previously been measured to be 0.70 ps (Ref. 12) (scattering rate of 1.43×10^{12} s^{-1}). From our measured densities we estimate that the $X_7 \rightarrow \Gamma$ intervalley scattering time is 0.60 ps (scattering rate of 1.70×10^{12} s^{-1}). Thus, $X_7 \rightarrow \Gamma$ intervalley scattering is about 1.2 times faster than $X_6 \rightarrow \Gamma$ intervalley scattering. This is in reasonable agreement with the theoretical deformation potential constant calculations of Zollner, Gopalan, and Cardona.[16] Finally, it can be seen from Fig. 1(b) that after 60 ps all the electrons have scattered out of the X valleys and the interconduction band absorption no longer exists.

In conclusion, using femtosecond UV-pump–IR-probe absorption spectroscopy to study the relaxation dynamics of high-energy, high-density electrons in GaAs, we have measured the energy-band renormalization of the X_6 and X_7, conduction-band valleys due to the presence of the high-density electron-hole plasma, performed the measurement of an X_7 valley involved intervalley scattering, measured the effect of the high density of electrons on the energy relaxation through this channel, and determined the intervalley scattering time for $X_7 \rightarrow \Gamma$ to be faster than that for $X_6 \rightarrow \Gamma$. This study is most important for understanding electron transport in high-speed, high-field devices.

We would like to thank Dr. N. Ockman for helpful discussions. This research was supported by the Army Research Office.

[1]K. Berthold, A. F. J. Levi, J. Walker, and R. J. Malik, Appl. Phys. Lett. **54**, 813 (1989).

[2]T. González Sánchez, J. E. Velázquez Pérez, P. M. Gutiérrez Conde, and D. Pardo Collantes, Semicond. Sci. Technol. **6**, 862 (1991).

[3]H. Haug and S. Schmitt-Rink, Prog. Quantum Electron. **9**, 3 (1984).

[4]W. F. Brinkman and T. M. Rice, Phys. Rev. B **7**, 1508 (1973).

[5]C. V. Shank, R. L. Fork, R. F. Leheny, and J. Shah, Phys. Rev. Lett. **42**, 112 (1979).

[6]K. Bohnert, H. Kalt, A. L. Smirl, D. P. Norwood, T. F. Boggess, and I. J. D'Haenens, Phys. Rev. Lett. **60**, 37 (1988).

[7]H. Kalt and M. Rinker, Phys. Rev. B **45**, 1139 (1992).

[8]J. Pankove, *Optical Processes in Semiconductors* (Dover, New York, 1971), Chap. 3.

[9]W. B. Wang, Kai Shum, R. R. Alfano, D. Szmyd, and A. J. Nozik, Phys. Rev. Lett. **68**, 662 (1992).

[10]W. W. Ruhle, K. Leo, and E. Bauser, Phys. Rev. B **40**, 1756 (1989).

[11]A. S. Jordan, J. Appl. Phys. **51**, 2218 (1980).

[12]W. B. Wang, N. Ockman, M. A. Cavicchia, M. Yan, and R. R. Alfano, Proc. SPIE **1282**, 285 (1990).

[13]V. C. Aguilera-Navarro, G. A. Estévez, and Allyn Kostecki, J. Appl. Phys. **63**, 2848 (1988).

[14]M. Capizzi, S. Modesti, A. Frova, J. L. Staehli, M. Guzzi, and R. A. Logan, Phys. Rev. B **29**, 2028 (1984).

[15]P. Vashishta and R. K. Kalia, Phys. Rev. B **25**, 6492 (1982).

[16]S. Zollner, S. Gopalan, and M. Cardona, Appl. Phys. Lett. **54**, 614 (1989).